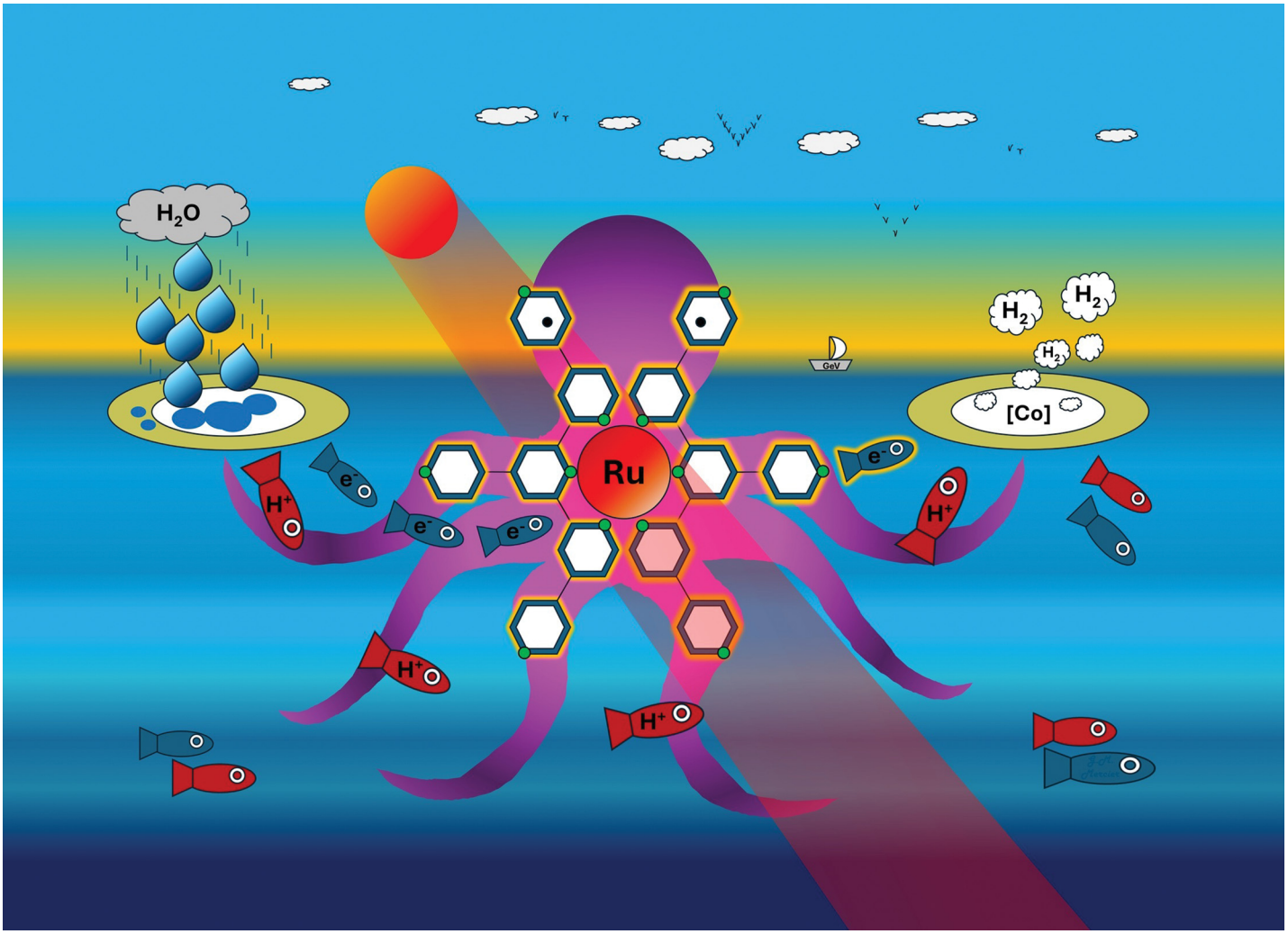

Showcasing research from Professor Hanan's laboratory, School of Chemistry, University of Montreal, Québec, Canada.

A ruthenium terpyridine complex showing stable photocatalytic hydrogen evolution under red light

We report herein the synthesis of a novel terpyridine ruthenium(II) complex, which shows stable hydrogen photoproduction under red light over more than nine days. A sustained activity under blue and green lights is also observed over more than seven days.

Image reproduced by permission of Gabriel Mercier from *Chem. Commun.*, 2025, **61**, 14911.

As featured in:

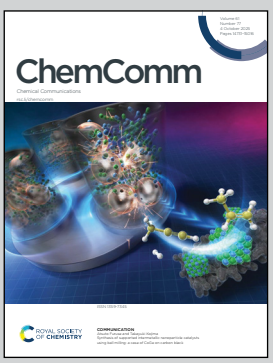

See Valérie Marvaud, Garry S. Hanan *et al.*, *Chem. Commun.*, 2025, **61**, 14911.

ROYAL SOCIETY OF CHEMISTRY

rsc.li/chemcomm

Registered charity number: 207890

ChemComm

COMMUNICATION

View Article Online
View Journal | View Issue

Cite this: *Chem. Commun.*, 2025, **61**, 14911

Received 28th July 2025,
Accepted 18th August 2025

DOI: 10.1039/d5cc04303d

rsc.li/chemcomm

A ruthenium terpyridine complex showing stable photocatalytic hydrogen evolution under red light†

Gabriel M. Mercier, ‡[a] Elodie Rousset, ‡[ab] Ilyes Oubaha,[a] Kamalika Bandyopadhyay,[c] Amlan K. Pal,[c] Ilaria Ciofini,[d] Lise-Marie Chamoreau,[b] Valérie Marvaud*[b] and Garry S. Hanan *[a]

We report herein the synthesis of a tridentate ligand (tris-4,4′,4″-(4‴-pyridyl)-2,2′:6′,2″-terpyridine) and its corresponding homoleptic ruthenium(II) complex, which shows stable hydrogen photoproduction under red light (TON of 174 mol_{H_2} mol_{PS}^{-1} after 210 hours). A sustained activity under blue and green lights is also observed with TONs above 360 mol_{H_2} mol_{PS}^{-1} after 168 hours.

For decades ruthenium polypyridyl complexes have attracted considerable interest thanks to their useful optical properties, *e.g.*, visible light absorption and long-lived excited states, and ease of incorporation into artificial light-harvesting systems.[1,2] While myriad mononuclear complexes have been reported in the literature,[3] research has also focused on the construction of bigger assemblies incorporating one or more desired functionalities introduced by specific building blocks.[4–7] Recently, an exceptional organic photosensitizer with high efficiency has been reported, however, this system still has a lack of long-term stability which needs to be addressed.[8] Other recent routes include the development of quantum dots using non-noble metals with recently reported turn-over frequency (TOF) reaching 200 mol_{H_2} mol_{PS}^{-1} h^{-1} under red-light.[9] Still, ruthenium based complexes shows very high activity under various wavelengths, for instance up to 2100 mol_{H_2} mol_{PS}^{-1} h^{-1} under blue light.[10] Being able to tune such ruthenium complexes in order to have panchromatic efficiency, along with an increase in stability, is now a requirement. As a result, the design of the ligand has become more important as it acts both as a structural element and influences the properties of the final complex.[11–15] By analogy with the 2,2′:4,4″:4′,4″ quaterpyridine (qpy) and its ruthenium complexes,[16] we report here the first synthesis and recorded properties of the tris 4,4′,4″-(4‴-pyridyl)-2,2′:6′,2″-terpyridine (py_3tpy) ligand and its homoleptic Ru(II) complex. Considering the vast literature of 4,4′-bipyridine (4,4′-bpy), qpy and 2,2′:6′,2″-terpyridine (tpy) itself, the absence of this fundamental py_3tpy is surprising. Even if the properties of $[Ru(tpy)_2]^{2+}$ complex are deactivated by a thermally populated ^{3}MC state compared to its bidentate analogue $[Ru(bpy)_3]^{2+}$,[1] it presents the major advantage of being achiral in its metal complexes of octahedral coordination geometry. Therefore, terpyridine-based complexes don't present Δ and Λ enantiomers which in turn reduces the number of diastereotopic isomers produced when building polynuclear architectures.[1] The py_3tpy terpyridine derivative herein presents four coordination sites: a core *N^N^N* tridentate one, allowing for a strong chelate effect, and three *N*-coordinating monodentate peripheral centers. This feature can thus enable the formation of functional multinuclear architectures, for example linking a photosensitizer with a catalyst, such as $[Co^{III}(dmgH)_2(py)Cl]$, for hydrogen production.[16,17]

The synthesis of the ligand is based on a common approach derived from the Kröhnke pyridine synthesis method[18] and widely used in our group.[19] It consists in forming the central ring from two equivalents of acetylated derivatives and one aldehyde, in the presence of ammonium ions. The py_3tpy ligand is therefore obtained from commercial 4-pyridine-carboxaldehyde and 2-acetyl-4,4′-bipyridine, synthesized according to the procedure developed in our group.[20] Two py_3tpy ligands are then reacted with $[Ru(DMSO)_4Cl_2]$, yielding the homoleptic complex $[Ru(py_3tpy)_2]^{2+}$ isolated as the hexafluorophosphate salt (Scheme 1). Further synthetic details are available in section S1 in the SI, along with NMR (SI, S2a), IR (SI, S2b), and HR-MS characterization.

Dark red crystals of the complex were grown by slow diffusion of diethyl ether into an acetone solution of the compound, allowing single crystal X-Ray diffraction (XRD) characterization of a solvated $[Ru(py_3tpy)_2](PF_6)_2$. The corresponding structure is presented in Fig. SI.9. The complex crystallizes in $P2_1/n$ monoclinic space group. The asymmetric unit contains one molecule of the complex, two molecules of PF_6^- as well as one molecule

[a] *Département de Chimie, Université de Montréal, Montréal, Québec H3C 3J7, Canada. E-mail: garry.hanan@umontreal.ca*
[b] *IPCM-CNRS UMR 8232, Sorbonne University, cc 229, 4 place Jussieu, 75252 Paris Cedex 05, France. E-mail: valerie.marvaud@sorbonne-universite.fr*
[c] *Department of Chemistry, Indian Institute of Technology Jammu, Nagrota Bypass Road, Jammu and Kashmir-181221, India*
[d] *i-CLeHS, PSL UMR 8060, 11 rue Pierre et Marie Curie, 75005 Paris, France*
† The authors thank T. Biellmann for his initial effort in this project.
‡ These authors contributed equally.

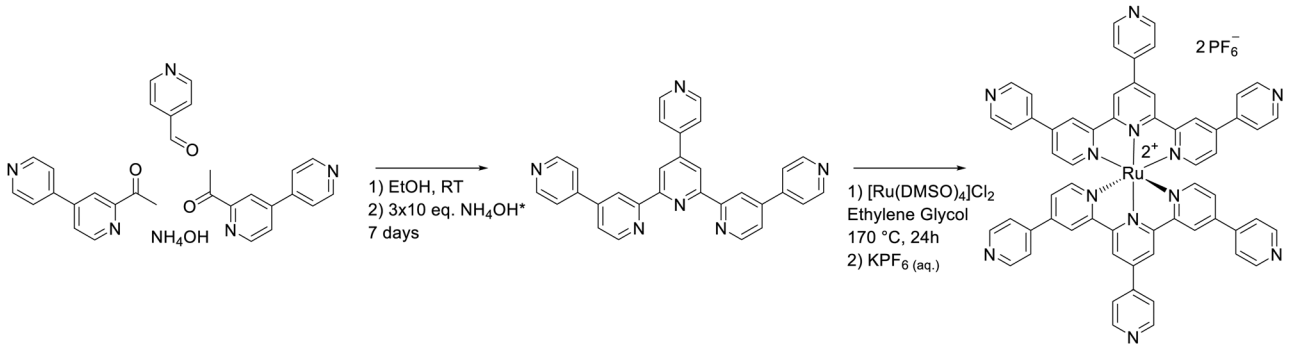

Scheme 1 Synthesis of the py_3tpy ligand and corresponding $[Ru(py_3tpy)_2](PF_6)_2$ complex. *See SI for further details.

of water, diethyl ether and acetone. The compound shows a distorted octahedral geometry of the ruthenium coordination sphere, with *trans* N–Ru–N angles of both tpy *ca.* 157.4 ± 0.1°, characteristic of terpyridine ligands.[15] Each py_3tpy ligand exhibits torsion angles of the outer pyridines between 11 and 38°, similar to previously reported ones,[16] and a flatness of the terpyridine sites (average angle between pyridine planes < 1°). The variation in the torsion angles of the pyridines observed in the XRD structure may arise from the involvement of the outer pyridines in π-stacking interactions occurring in the solid state.

The redox behavior of the complex was examined by cyclic voltammetry (CV). The CV (SI Fig. S7) typically shows a one-electron reversible oxidation wave attributed to the Ru^{2+}/Ru^{3+} couple at 1.38 V *vs.* SCE. On the reduction side, two well-defined reversible waves, attributed to the sequential one-electron reductions of the py_3tpy ligands, are observed at −1.07 and −1.22 V *vs.* SCE. DFT calculations also supports the attribution as the HOMO (highest occupied molecular orbital) and LUMO (lowest unoccupied molecular orbital) reside predominantly on the Ru(II) and the tpy core, respectively (Fig. 1). Compared to the archetypical $[Ru(tpy)_2](PF_6)_2$, and similarly to previously reported $[Ru(qpy)_3](PF_6)_2$,[16] $[Ru(py_3tpy)_2](PF_6)_2$ is, therefore, harder to oxidize and easier to reduce (Table 1), in accordance with the increased withdrawing effect of a pendant pyridyl group as compared to simple hydrogen substituent.

The synthesized complex presents a low energy absorption band centered at 500 nm (Fig. 2) classically attributed to a metal-to-ligand charge-transfer (MLCT) transition along with a series of bands at higher energy, attributed to ligand-centered (LC) transitions.[1,2] The ^{1}MLCT nature of the bands at 500 nm and ∼370 nm (sh) was further supported by TD-DFT calculations with oscillator strength of >0.07. The band at ∼340 nm is an admixture of ^{1}LC (major) and ^{1}MLCT (minor) transitions.

The complex presents a bathochromic shift of 25 nm and 27 nm compared to $[Ru(tpy)_2]^{2+}$,[22] and $[Ru(qpy)_3]^{2+}$,[16] complexes, respectively. This is also supported by lower HOMO–LUMO gap calculated for $[Ru(py_3tpy)_2](PF_6)_2$ than that of $[Ru(tpy)_2](PF_6)_2$ (Table 2). This shift is noteworthy for solar hydrogen evolution as it aligns with the peak of the solar emission spectrum received at the sea level, also centered at 500 nm.[23]

The $[Ru(py_3tpy)_2](PF_6)_2$ complex exhibits luminescence properties at room temperature, characterized by a ^{3}MLCT emission

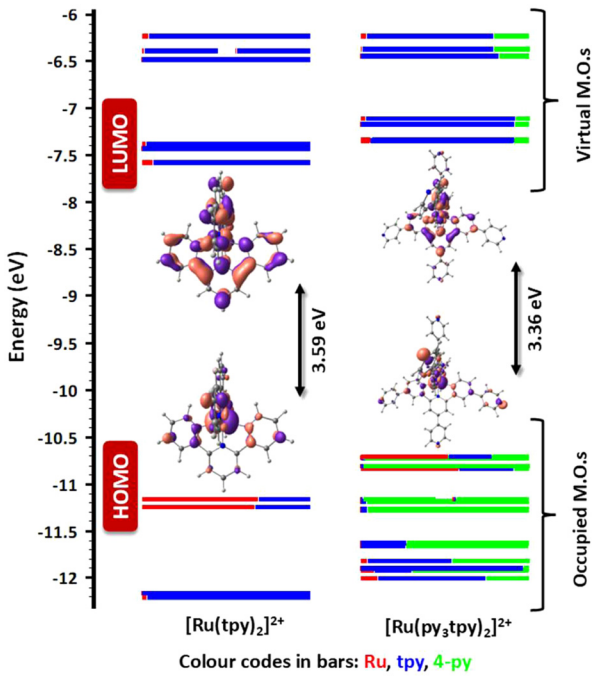

Fig. 1 Calculated energy level diagram and Kohn–Sham M. O. S of $[Ru(tpy)_2]^{2+}$ and $[Ru(py_3tpy)_2]^{2+}$ (B3LYP/6-31G** for C, H, N and SBKJC-VDZ for Ru). Density maps are iso-contoured at 0.03.

Table 1 Electrochemical data of the $[Ru(py_3tpy)_2]^{2+}$, $[Ru(tpy)_2]^{2+}$and $[Ru(qpy)3]^{2+}$ complexes

Complex	$E^{ox}_{1/2}$ (V)[a]	$E^{red1}_{1/2}$ (V)[a]	$E^{red2}_{1/2}$ (V)[a]	Band gap (V)
$[Ru(py_3tpy)_2]^{2+}$	1.38 (107)	−1.07 (81)	−1.22 (86)	2.45
$[Ru(tpy)_2]^{2+}$,[21]	1.30	−1.24	−1.49	2.54
$[Ru(qpy)_3]^{2+}$,[16]	1.48 (77)	−0.99 (63)	−1.14 (66)	2.47

[a] Potentials are given in volts *vs.* SCE in acetonitrile at 100 mV s^{-1}, room temperature and with $TBAPF_6$ (0.1 M) as supporting electrolyte. The difference between cathodic and anodic peak potentials, ΔE_p, (millivolts) is given in parentheses.

centered at 670 upon excitation at 500 nm (Fig. 2), a quantum yield of 0.6% and lifetime of 5 ns (Table 2). Interestingly, the complex has a significant bathochromic shift of 50 nm compared to $[Ru(bpy)_3]^{2+}$,[24,25] and has a higher quantum yield and lifetime than its analogue $[Ru(tpy)_2]^{2+}$.[22] The predicted

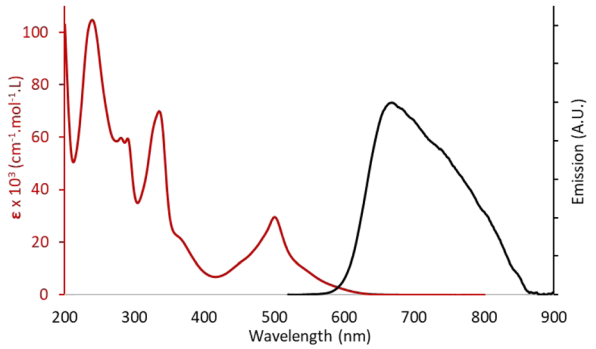

Fig. 2 Absorption (red) and normalized emission (black) spectra of the $[Ru(py_3tpy)_2](PF_6)_2$ in acetonitrile.

Table 2 Emission data of $[Ru(py_3tpy)_2]^{2+}$, $[Ru(tpy)_2]^{2+}$, $[Ru(bpy)_3]^{2+}$, and $[Ru(qpy)_3]^{2+}$ in degassed acetonitrile

Complex	$\lambda_{max\,abs}$ (nm)	ε (L mol^{-1} cm^{-1})	λ_{em} (nm)	Φ (%)	τ (ns)
$[Ru(py_3tpy)_2]^{2+}$	500	3.0×10^4	670	0.6	5
$[Ru(tpy)_2]^{2+}$,[22]	475	1.6×10^4	630	<0.001	0.3
$[Ru(bpy)_3]^{2+}$,[24,25]	450	1.8×10^4	610	9.5	870
$[Ru(qpy)_3]^{2+}$,[16]	473	2.9×10^4	628	23	1780

emission maximum, $E_{AE} = E(T_1) - E(S_0)$, at the T_1 optimized geometries (adiabatic electronic emission) obtained by DFT calculations for $[Ru(py_3tpy)_2]^{2+}$ was found to be at 646 nm, and match closely those observed experimentally and also fall in agreement with the observed trend of red-shifted emission maxima from $[Ru(tpy)_2]^{2+}$ to $[Ru(py_3tpy)_2]^{2+}$. The predicted emission maximum was calculated with a relative error of 3% for $[Ru(py_3tpy)_2]^{2+}$, using the equation error = $|[(\lambda_{PL}(298\ K) - E_{AE})]/\lambda_{PL}(298\ K)|$ in eV. Thus, these properties make it a suitable candidate as a building block for artificial photosynthesis applications harvesting red solar wavelengths.

The potential for light-driven hydrogen production of the $[Ru(py_3tpy)_2](PF_6)_2$ complex was evaluated at different wavelengths (blue – 445 nm, green – 495 nm, and red – 630 nm) under the following photocatalytic conditions: DMF as solvent, triethanolamine (TEOA) as a sacrificial electron donor, HBF_4 as a proton donor and cobaloxime $[Co^{III}(dmgH)_2(py)Cl]$ as a catalyst. As panchromaticity is of high interest for further artificial photosynthesis applications, the three wavelengths used within this work were selected to cover most of the visible part of the solar emission spectrum.

Similarly to previously published modified terpyridine complexes,[20] the new photosensitizer shows sustained hydrogen production for more than seven days under blue and green lights and complete stability over more than 9 days under red light (Fig. 3). To compare, the well-known $[Ru(bpy)_3](PF_6)_2$ and $[Ru(ttpy)_2](PF_6)_2$ (Ref. 26) complexes were also measured in the same conditions.

The induction time is very short for blue and green lights: hydrogen production is observed within five minutes after switching on the lamp for both $[Ru(py_3tpy)_2](PF_6)_2$ and $[Ru(bpy)_3](PF_6)_2$ complexes. The maximum TOF are reached after around five minutes and one hour for blue and green light, respectively. Under red light the induction time was around two hours for $[Ru(py_3tpy)_2](PF_6)_2$. It took several days for the TOF to reach its maximum value in as shown in Fig. 3 while no quantifiable amount of hydrogen (below 0.2 mol_{H_2} mol_{PS}^{-1} h^{-1}) could be observed for $[Ru(bpy)_3](PF_6)_2$.

Under blue light the system already shows enhanced stability when compared to $[Ru(bpy)_3](PF_6)_2$ complex: the TOF remained at around 44% of its maximum value after around 168 h with a TON of 376 mol_{H_2} mol_{PS}^{-1} at that point whereas $[Ru(bpy)_3](PF_6)_2$ complex stopped producing hydrogen after around 32 hours with a TON of 1473 mol_{H_2} mol_{PS}^{-1} (Fig. 3). No hydrogen production was observed for the $[Ru(ttpy)_2](PF_6)_2$ complex. The hydrogen quantum yield for the maximum TOF of $[Ru(py_3tpy)_2]^{2+}$ reached φ_{rH_2} = 0.15% (24% for $[Ru(bpy)_3]^{2+}$) and for the complete photoreaction φ_{rH_2} = 0.09% (0.83% for $[Ru(bpy)_3]^{2+}$).

Under green light, the gain in stability is more pronounced with a TOF at around 63% of its maximal value after 168 h and TON of 361 $mmol_{H_2}$ mol_{PS}^{-1} at that point, while $[Ru(bpy)_3](PF_6)_2$ complex stopped producing hydrogen after 60 h with a TON of 1330 mol_{H_2} mol_{PS}^{-1} (Fig. 3) and no hydrogen production was observed for the $[Ru(ttpy)_2](PF_6)_2$ complex. The hydrogen quantum yield for the maximum TOF of $[Ru(py_3tpy)_2]^{2+}$

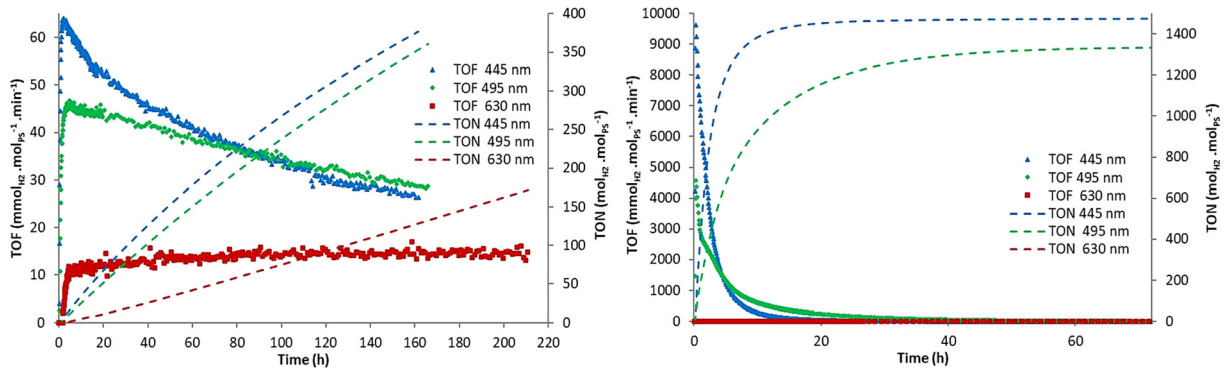

Fig. 3 TOF and TON evolution over time for $[Ru(py_3tpy)_2](PF_6)_2$ (left) and $[Ru(bpy)_3](PF_6)_2$ (right) at 630 nm (red curves), 495 nm (green curves) and 445 nm (blue curves) with a 50 mW LED.

reached φ_{rH_2} = 0.11% (11% for $[Ru(bpy)_3]^{2+}$) and for the complete photoreaction φ_{rH_2} = 0.08% (0.78% for $[Ru(bpy)_3]^{2+}$).

Under red light, the system shows long-term stability and a TON of 174 mol_{H_2} mol_{PS}^{-1} after 210 h. The TOF under red light reached a maximum value after approximately 80 h and remained constant at around 0.84 mol_{H_2} mol_{PS}^{-1} h^{-1} for at least another 130 h. As a comparison, the well-known $[Ru(bpy)_3](PF_6)_2$ complex only shows detectable but not quantifiable hydrogen production under the same conditions (see SI for limit of detection and quantification calculations), while previously reported $[Ru(qpy)_3]^{2+}$ shows high activity, reaching a TON of 375 mol_{H_2} mol_{PS}^{-1} after 20 h, but displaying low stability as the TOF was cut in four within that timeframe.[16] The hydrogen quantum yield for the maximum TOF of $[Ru(py_3tpy)_2]^{2+}$ reached φ_{rH_2} = 0.025% and for the complete photoreaction φ_{rH_2} = 0.020%.

At the end of the measurements, additional experiments were carried out with the addition of cobaloxime, TEOA, HBF_4 and photosensitizer solutions, as well as solvent. As previously reported for other ruthenium photosensitizers in literature,[20] only the extra additions of photosensitizer solution led to a revival of hydrogen production. This finding indicates that the observed decline in hydrogen production results from the decomposition of the photosensitizer throughout the experiments.

In summary, we report herein a newly synthesized py_3tpy ligand, readily forming its corresponding homoleptic ruthenium(II) complex under standard thermal synthesis. In HER experiment, this complex shows hydrogen production under blue and green wavelengths while displaying a remarkable stability for more than nine days under red light irradiation. At the 210 hours mark, the complex achieved a TON of 174 mol_{H_2} mol_{PS}^{-1} (about 12% of the maximal TON reached by the archetypal $[Ru(bpy)_3]^{2+}$ complex under blue light) with hydrogen production continuing. Stability, which is a key requirement for future applications in artificial photosynthesis and industrial hydrogen production, has been achieved here under red light with the newly synthetized py_3tpy ligand and its corresponding homoleptic ruthenium complex.

The research has been supported by the CNRS, UPMC (University Pierre et Marie Curie), the French Ministry of Research, ANR (Switch-2010-Blan-712), ANR E-storic (14-CE05-0002), MITACS Globalink Research Award – Sorbonne Université, the Fonds de Recherche du Québec – Nature et Technologies (FRQNT) and the Natural Sciences and Engineering Research Council (NSERC) of Canada. ER thanks the chemistry department of University of Montréal, FRQNT and NSERC for financial support. GMM thanks Wallonie-Bruxelles International (WBI) for financial support. AKP thanks the RSC Researcher Collaborations Grant (C24-7343877336). Access to the NMR *via* the Regional Centre for Magnetic Resonance (UdeM – Chemistry) was possible due to funding from the Canada Foundation for Innovation and the Institute Courtois.

Conflicts of interest

There are no conflicts to declare.

Data availability

Synthesis, methods, characterization, and crystallographic data. See DOI: https://doi.org/10.1039/d5cc04303d

CCDC 2476596 contains the supplementary crystallographic data for this paper.[27]

Notes and references

1 S. Campagna, F. Puntoriero, F. Nastasi, G. Bergamini and V. Balzani, *Top. Curr. Chem.*, 2007, **280**, 117–214.
2 O. A. Borg, S. S. M. C. Godinho, M. J. Lundqvist, S. Lunell and P. Persson, *J. Phys. Chem. A*, 2008, **112**, 4470–4476.
3 D. G. Giarikos, *Natural and Artificial Photosynthesis*, John Wiley & Sons, Inc, Fort Lauderdale, 2013, 143–171.
4 H. Ozawa, M. Haga and K. Sakai, *J. Am. Chem. Soc.*, 2006, **128**, 4926–4927.
5 P. Ceroni, A. Credi, M. Venturi and V. Balzani, *Photochem. Photobiol. Sci.*, 2010, **9**, 1561–1573.
6 S. Bonnet, J.-P. Collin and J.-P. Sauvage, *Chem. Commun.*, 2005, 3195–3197.
7 B. Laramée-Milette, F. Nastasi, F. Puntoriero, S. Campagna and G. S. Hanan, *Chem. – Eur. J.*, 2017, **23**, 16497–16504.
8 M. Ming, H. Yuan, S. Yang, Z. Wei, Q. Lei, J. Lei and Z. Han, *J. Am. Chem. Soc.*, 2022, **144**, 19680–19684.
9 Z. Wei, S. Yang, J. Lei, K. Guo, H. Yuan, M. Ming, J. Du and Z. Han, *Chem. – Eur. J.*, 2024, **30**, 1–5.
10 O. Schott, A. K. Pal, D. Chartrand and G. S. Hanan, *ChemSusChem*, 2017, **10**, 4436–4441.
11 T. Jin, D. Wagner and O. S. Wenger, *Angew. Chem., Int. Ed.*, 2024, **63**, 1–12.
12 J. Moll, C. Förster, A. König, L. M. Carrella, M. Wagner, M. Panthöfer, A. Möller, E. Rentschler and K. Heinze, *Inorg. Chem.*, 2022, **61**, 1659–1671.
13 M. Abrahamsson, M. Jäger, J. H. Kumar, T. Österman, P. Persson, H.-C. Becker, O. Johansson and L. Hammarström, *J. Am. Chem. Soc.*, 2008, **130**, 15533–15542.
14 A. K. Pal, S. Serroni, N. Zaccheroni, S. Campagna and G. S. Hanan, *Chem. Sci.*, 2014, **5**, 4800–4811.
15 M. T. Rupp, N. Shevchenko, G. S. Hanan and D. G. Kurth, *Coord. Chem. Rev.*, 2021, **446**, 214127–214142.
16 E. Rousset, D. Chartrand, I. Ciofini, V. Marvaud and G. S. Hanan, *Chem. Commun.*, 2015, **51**, 9261–9264.
17 M. Razavet, V. Artero and M. Fontecave, *Inorg. Chem.*, 2005, **44**, 4786–4795.
18 F. Kröhnke, *Synthesis*, 1976, 1–24.
19 J. Wang and G. S. Hanan, *Synlett*, 2005, 1251–1254.
20 M. Rupp, T. Auvray, E. Rousset, G. M. Mercier, V. Marvaud and G. S. Hanan, *Inorg. Chem.*, 2019, **58**, 9127–9134.
21 Y.-Q. Fang, N. J. Taylor, F. Laverdière, G. S. Hanan, F. Loiseau, F. Nastasi, S. Campagna, H. Nierengarten, E. Leize-Wagner and A. V. Dorsselaer, *Inorg. Chem.*, 2007, **46**, 2854–2863.
22 C. R. Hecker, A. K. I. Gushurst and D. R. McMillin, *Inorg. Chem.*, 1991, **30**, 538–541.
23 L. Wang and J. Yu, *Principles of Photocatalysis, S-scheme Heterojunction Photocatalysts*, Academic Press, Wuhan, 2023, 1–50.
24 A. Juris, V. Balzani, F. Barigelletti, S. Campagna, P. Belser and A. von Zelewsky, *Coord. Chem. Rev.*, 1988, **84**, 85–277.
25 K. Suzuki, A. Kobayashi, S. Kaneko, K. Takehira, T. Yoshihara, H. Ishida, Y. Shiina, S. Oishi and S. Tobita, *Phys. Chem. Chem. Phys.*, 2009, **11**, 9850–9860.
26 K. E. Spettel and N. H. Damrauer, *J. Phys. Chem. A*, 2014, **118**, 10649–10662.
27 G. M. Mercier, E. Rousset, I. Oubaha, K. Bandyopadhyay, A. K. Pal, I. Ciofini, L.-M. Chamoreau, V. Marvaud and G. S. Hanan, CCDC 2476596: Experimental Crystal Structure Determination, 2025, DOI: 10.5517/ccdc.csd.cc2p4365.

